SCIENCE CHINA
Information Sciences

• RESEARCH PAPER •

December 2016, Vol. 59 122303:1–122303:12
doi: 10.1007/s11432-015-5493-5

Generalized spatial representation for digital modulation and its potential application

Hao HUAN[1,2*], Pengfei SHI[1], Xiaodong YAN[1] & Ran TAO[1]

[1]*School of Information and Electronics, Beijing Institute of Technology, Beijing* 100081*, China;*
[2]*Key Lab for Spacecraft TT&C and Communication under the Ministry of Education, Chongqing* 400044*, China*

Received August 10, 2015; accepted October 20, 2015; published online June 12, 2016

Abstract Constellation mapping has provided a great convenience to measure the performance of digital signal modulation in Euclid space. However, traditional in-phase and quadrature (IQ) plane is difficult to express the frequency modulation scheme such as minimum shift keying (MSK) and the time domain modulation such as cyclic code shift keying (CCSK). How to represent the digital signal modulation visually through constellation mapping is an attractive problem. To address this issue, in this paper, the combined frequency and phase modulation are utilized to define a new kind of constellation mapping, where the phase and frequency are quantized to the same elements. The uniform geometric construction for combined phase and frequency modulation is redefined in the 3D cylindrical coordinate system based on frequency ($\boldsymbol{f}$), in-phase component ($\boldsymbol{I}$) and quadrature component ($\boldsymbol{Q}$). In the new coordinates, the quadrature frequency-phase shift keying (QFPSK) is produced by the QPSK with dimensional rotation matrix and denoted by the reduced dual quaternion. Furthermore, the spatial extension from QFPSK to chirp cyclic shift keying (Chirp CSK) is analyzed with bandwidth efficiency and energy efficiency. At last, the QFPSK is combined with the 2D OFDM, yielding the image OFDM system. Experimental results verify the effectiveness of QFPSK in the proposed system with the time-varying wireless channel and frequency selective fading channel respectively.

Keywords quadrature frequency-phase shift keying (QFPSK), chirp cyclic shift keying, spatial constellation mapping, image OFDM system, wireless communication

Citation Huan H, Shi P F, Yan X D, et al. Generalized spatial representation for digital modulation and its potential application. Sci China Inf Sci, 2016, 59(12): 122303, doi: 10.1007/s11432-015-5493-5

1 Introduction

The dimensions of signal modulation are an efficient way to improve the transmission efficiency according to Shannon theorem. It is stated in [1] that the number of signal dimensions is well approximated by twice the time-bandwidth product. The signal space has been proved to enhance the transmission gain deeply by either the extension of dimension (time [2] and frequency extension [3]), or the inner multidimensional rotation (phase extension) [4]. Then, the quadrature-quadrature phase-shift keying was first proposed by combining them together in [5], where the available signal space is utilized more efficiently than traditional two dimensional schemes such as quadrature frequency-phase shift keying (QPSK) and minimum shift keying (MSK). These methods have been applied to increase the transmission

* Corresponding author (email: huanhao@bit.edu.cn)

© Science China Press and Springer-Verlag Berlin Heidelberg 2016

performance in communication system. For instance, the construction of high level lattice 3D constellation mapping was introduced to the orthogonal frequency division multiplexing (OFDM) system to obtain low symbol error probabilities [6]. Meanwhile, the multidimensional rotation has been used in multiple-input multiple-output (MIMO) system [7] to reach the maximum diversity gain. Furthermore, the code design and capacity for combined frequency and phase modulation called continuous-phase frequency shift keying (CPFSK) have been described in [8, 9].

However, most of researchers have just focused on designing different modulations but ignored the relationship between geometrical structure and physical significance in wireless communication, such as the distinction and connection between phase and frequency. To the authors' best knowledge, the intrinsic geometric structure called information geometry has not been used to unify phase and frequency modulation. Besides, the mathematical expression for combined phase and frequency modulation also remains for further investigation.

In [10], we have preliminarily designed the 3D cylindrical coordinate system composed by frequency ($\boldsymbol{f}$), in-phase ($\boldsymbol{I}$) and quadrature phase ($\boldsymbol{Q}$) to unify the phase and frequency modulation. In this paper, the quantitative representation for 3D coordinates is obtained by the minimum Euclidean distance (MED) of frequency shift keying (FSK) and phase shift keying (PSK). In the proposed coordinate, the basic combined phase and frequency modulation called quadrature frequency-phase shift keying (QFPSK) is obtained from QPSK by the dimensional rotation matrix. Then, the reduced dual quaternion is used as the mathematical expression of QPFSK to distinguish the phase and frequency. Just like the extension from QPSK to MSK, the spatial extension from QFPSK to chirp cyclic shift keying (Chirp CSK) is analyzed in the cylindrical coordinate system with bandwidth efficiency and energy effciency. Finally, the QFPSK is combined with the 2D OFDM system, which reveals the inner relationship between image and communication.

The rest of this paper continues with the description of 3D coordinate system for unifying phase and frequency modulation, expressed by the reduced dual quaternion in Section 2. Then, the spatial extension from QFPSK to Chirp CSK is analyzed in Section 3. The QFPSK is introduced to the OFDM system with the properties of image in Section 4. Section 5 makes the conclusion.

2 Generalized constellation representation

In traditional modulation system, the constellation of multiple phase shift keying (MPSK) and multiple quadrature amplitude modulation (MQAM) is composed by a series of quadrature frequency-phase shift keying (QPSK). However, without the corresponding coordinate system, it is invalid to represent the spatial structure of combined frequency and phase modulation, such as MFSK and OFDM in traditional in-phase and quadrature (IQ) plane.

It is assumed that the input binary data stream $a(t)$ with the bit rate $1/T_b$ is demultiplexed into two streams $a_1(t)$ and $a_2(t)$, modulated by the QPSK signal $S_{\mathrm{qpsk}}(t)$:

$$\begin{aligned} S_{\mathrm{qpsk}}(t) &= \frac{1}{\sqrt{2T_b}} a_1(t) \cos(2\pi f_c t) + \frac{1}{\sqrt{2T_b}} a_2(t) \sin(2\pi f_c t) \\ &= \frac{1}{\sqrt{2T_b}} (a_1(t) \;\; a_2(t)) \begin{bmatrix} \cos(2\pi f_c t) \\ \sin(2\pi f_c t) \end{bmatrix}, \end{aligned} \tag{1}$$

where each of $a_1(t)$ and $a_2(t)$ is either 1 or -1.

According to the element decomposition of MPSK and MQAM, the concept of frequency and phase decomposition is introduced to the combined frequency and phase modulation. The modulation process is described by a $M_1 \otimes M_2$ tensor product (called Kronecker product), where M_1 and M_2 denote the number of carrier frequencies and phases respectively. Similar to QPSK as the basic component of MPSK and MQAM, the $2 \otimes 2$ tensor product is regarded as the basic component of the general $M_1 \otimes M_2$ frequencies

and phases modulation, called quadrature frequency-phase shift keying (QFPSK).

$$S_{\text{qfpsk}}(t) = \frac{1}{\sqrt{2T_b}}(a_1(t)\ \ a_2(t)) \begin{bmatrix} \cos\dfrac{\pi t}{2T_b} & -\sin\dfrac{\pi t}{2T_b} \\ -\sin\dfrac{\pi t}{2T_b} & \cos\dfrac{\pi t}{2T_b} \end{bmatrix} \begin{bmatrix} \cos(2\pi f_c t) \\ \sin(2\pi f_c t) \end{bmatrix}$$
$$= \frac{1}{\sqrt{2T_b}}(a_1(t)\ \ a_2(t))\boldsymbol{R} \begin{bmatrix} \cos(2\pi f_c t) \\ \sin(2\pi f_c t) \end{bmatrix}, \tag{2}$$

where $\boldsymbol{R}$ denotes a general rotation matrix called dimensional rotation matrix. The dimensional rotation matrix transforms the QPSK with $1 \otimes 4$ to QFPSK with $2 \otimes 2$. It is noted that the dimension of both QPSK and QFPSK is 2, while the modulation mode is different. According to the waveform design in (2), the conception of new 3D coordinate system is first given in our previous paper [10] as follows.

Since the frequency can be regarded as a special phase, it is possible to unify frequency and phase together in a new coordinate system. In the given phase-frequency plane, the geometric space of frequency and phase modulation can be described as the tangent bundle of manifold with the tendency $f = f(t)$. The manifold just describes the relationship between IQ signal and the OFDM carriers. So first we could say that $f(t)$ is independent to IQ signal. Of course, the continuous frequency $f(t)$ could not be orthogonal to IQ plane, but luckily the discrete form can. As is known, the subcarriers in OFDM or MFSK are orthogonal for its discrete frequencies. Specially, taking the orthogonal 2FSK and QPSK in Figure 1 for example, we define the normalized MED to unite them together, called "generalized orthogonality". Under the generalized orthogonality, the new 3D coordinates based on $\boldsymbol{f}$, $\boldsymbol{I}$ and $\boldsymbol{Q}$ are generated by taking the traditional IQ modulation as a plane along the frequency line $\boldsymbol{f}$,

$$\begin{cases} \boldsymbol{I} = \cos 2\pi f_0 t, \\ \boldsymbol{Q} = \sin 2\pi f_0 t, \\ \boldsymbol{f} = f(t). \end{cases} \tag{3}$$

In [10], we only give the conceptual description of the 3D coordinate in (3). The purpose of the 3D coordinates is to unify the existing digital modulation together. We try to express the PSK and QAM at the baseband, as well as MSK, MFSK and chirp spectral spreading modulation under a normalized general Euclid distance. Meanwhile, the quantitative representation for the 3D coordinate is vital for further application. Thus in the following part, we will give the definition to obtain the unified phase and frequency modulation based on the Euclid distance of 2FSK and 2PSK.

2.1 Quantitative representation for 3D coordinates

The normalized MED provides a feasible way to establish the connection between frequency modulation and phase modulation as depicted in Figure 1. As a special case of OQPSK, traditional IQ plane is difficult to express the mapping scheme. Since the orthogonal projection of tetrahedron is the vertices of QPSK, the QFPSK based on the spatial rotation in Eq. (2) is given as follows.

As is known, the required signal noise ratio (SNR) of 2FSK is 3 dB higher than that of 2PSK to reach the same bit error rate (BER). The performance is measured by the normalized MED in Figure 1(a). The MED of orthogonal 2FSK is $d_{\Delta f} = \sqrt{2}$, while that of 2PSK is $d_{\Delta\phi} = 2$. Under the normalized MED, the QPSK and dual FSK are given in Figure 1(b). All of the four points are located in $\boldsymbol{fI}$ plane with the coordinate values: $(1, 0, \frac{\sqrt{2}}{2})$, $(-1, 0, \frac{\sqrt{2}}{2})$, $(1, 0, -\frac{\sqrt{2}}{2})$ and $(-1, 0, -\frac{\sqrt{2}}{2})$. The waveform design for dual FSK in Figure 1(b) is given by

$$\cos\left[2\pi\left(f_c + \frac{1}{4T_b}\right)t\right],\ -\cos\left[2\pi\left(f_c + \frac{1}{4T_b}\right)t\right],\ \cos\left[2\pi\left(f_c - \frac{1}{4T_b}\right)t\right],\ -\cos\left[2\pi\left(f_c - \frac{1}{4T_b}\right)t\right], \tag{4}$$

where f_c denotes the carrier frequency.

If two dual points at the same frequency plane f_0 in Figure 1(b) are changed from the direction of $\boldsymbol{I}$ to $\boldsymbol{Q}$, we obtain the QFPSK modulation with the increased Euclid distance in Figure 2(a). Thus, we

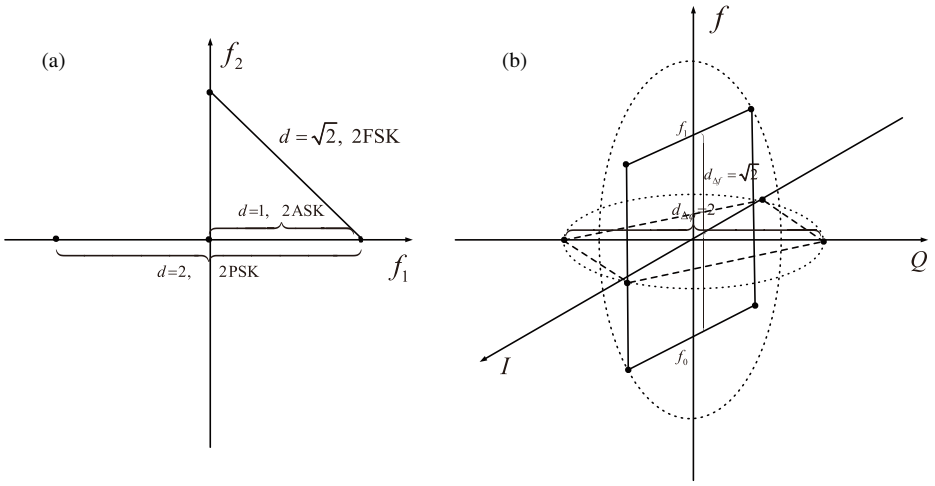

Figure 1 The 2D and 3D coordinate systems for phase and frequency modulation: (a) 2D coordinate system under normalized Euclid distance; (b) 3D coordinate system based on $\boldsymbol{f}$, $\boldsymbol{I}$ and $\boldsymbol{Q}$.

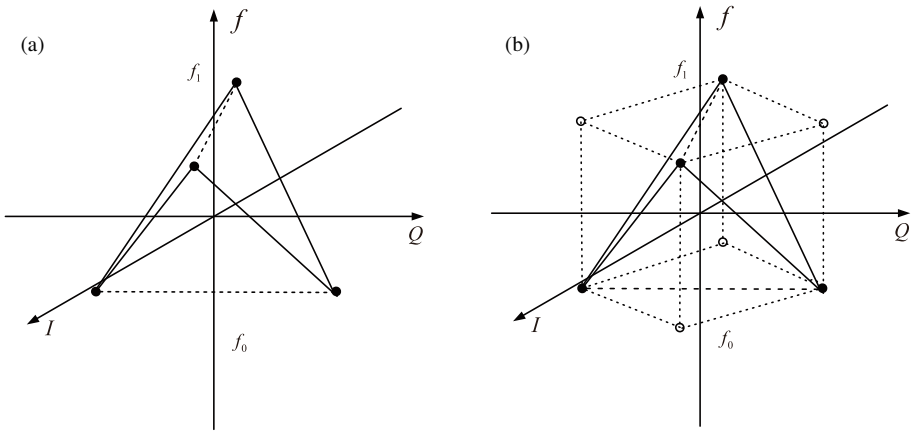

Figure 2 The special spatial structure for two kinds of 3D constellations: (a) $2 \otimes 2$ (QFPSK); (b) $2 \otimes 4$.

obtain the quantitative representation for 3D coordinates based on dimensional rotation matrix in (2). The coordinate values of the four points are $(1, 0, \frac{\sqrt{2}}{2})$, $(-1, 0, \frac{\sqrt{2}}{2})$, $(0, 1, -\frac{\sqrt{2}}{2})$ and $(0, -1, -\frac{\sqrt{2}}{2})$ with spherical coordinate system in [10], which form a regular tetrahedron together with the corresponding waveform,

$$\cos\left[2\pi\left(f_{\rm c}+\frac{1}{4T_b}\right)t\right],\ -\cos\left[2\pi\left(f_{\rm c}+\frac{1}{4T_b}\right)t\right],\ \sin\left[2\pi\left(f_{\rm c}-\frac{1}{4T_b}\right)t\right],\ -\sin\left[2\pi\left(f_{\rm c}-\frac{1}{4T_b}\right)t\right], \quad (5)$$

where $\int_{-T_b}^{T_b}\cos[2\pi(f_{\rm c}+\frac{1}{4T_b})t]\cdot\sin[2\pi(f_{\rm c}-\frac{1}{4T_b})t]{\rm d}t=0$ ensures the orthogonality of carriers. It is noted that the waveform in (5) is the combining form of the waveform design in [6].

The normalized MED between the points of QFPSK is the same with that of 2PSK, while that of QPSK is only $\sqrt{2}$ in Figure 2(a). If the problem of constant envelope is considered, the QFPSK is reduced to the MSK with the solid line path in Figure 2(a). It is claimed that the bit error rate (BER) of MSK is similar to BPSK and QPSK if the quadrature components are received by each matched filter respectively. In fact, the performance of BPSK and QPSK is better than that of MSK in additive white gaussian channel. The reason is illustrated by physical analysis rather than the mathematical derivation. As far as the authors' knowledge, the theoretical bit error rate (BER) of MSK is not given before. Here, based on the 3D coordinates, we give the theoretical BER of MSK.

According to the equivalent spatial structure of MSK in Figure 2(a), the decision region of MSK is an extended space of regular tetrahedron. According to [11], the symbol error rate of MSK is approximate

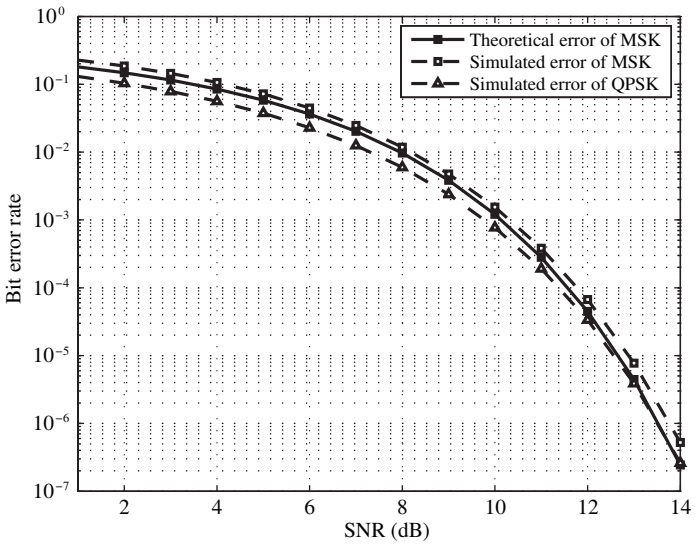

Figure 3 Theoretical bit error rate of MSK in AWGN.

to

$$P_s = 1 - \frac{1}{2}\mathrm{erfc}\left(-\frac{\sqrt{3}}{2\sigma}\right) + \frac{1}{4}\mathrm{erfc}\left(-\frac{\sqrt{3}}{4\sigma}\right)\exp\left(-\frac{9}{16\sigma^2}\right), \tag{6}$$

where $\mathrm{erfc}(\cdot)$ represents the complementary error function and σ^2 denotes the noise power. Thus, theoretical BER of MSK is

$$P_e = \frac{2^1}{2^2-1}P_s = \frac{2}{3}\left[1 - \frac{1}{2}\mathrm{erfc}\left(-\frac{\sqrt{3}}{2\sigma}\right) + \frac{1}{4}\mathrm{erfc}\left(-\frac{\sqrt{3}}{4\sigma}\right)\exp\left(-\frac{9}{16\sigma^2}\right)\right]. \tag{7}$$

The comparison between theoretical and simulated BER of MSK is given in normalized average energy in Figure 3. The theoretical result is matched with the simulated results in AWGN channel, which verifies the accuracy of the mathematical derivation for MSK. Three generalized neighbors (different phases and frequencies) around each vertex in Figure 2 just reduce the BER of MSK in low SNR, while they have little impact in high bit SNR. The theoretical value of BER for MSK just unites phase and frequency together, which reveals the real meaning of the 3D coordinates based on $\boldsymbol{f}$, $\boldsymbol{I}$ and $\boldsymbol{Q}$. The result further validates the feasibility assumptions for the 3D coordinate system.

Furthermore, on behalf of 3 bits modulation, the $2\otimes 4$ is divided into QFPSK and its dual form (hollow circles) in Figure 2(b). The $2\otimes 4$ structure is compatible with the 3 bit constant quadrature-quadrature phase-shift keying in [5].

2.2 Mathematical expression for QFPSK

The quaternion-valued modulation is used to modulate the signal across the two antennas to generate a 4D modulated signal in [12]. However, the quaternion can not be distinguished from different modulation mode, such as the different gain between antennas and QAM modulation. Besides, the quantitative relation between antennas and QAM is not given clearly in that paper. Here, the reduced dual quaternion is introduced to distinguish different modulation modes (phases and frequencies) and build the quantitative relation between them.

The mathematical expression for the symbol based on the biorthogonal carriers in frequency and phase is distinguished by the hypercomplex commutative algebra known as reduced dual quaternion,

$$S(t) = a(t) + b(t)\boldsymbol{i} + c(t)\boldsymbol{j} + d(t)\boldsymbol{k} = a(t) + b(t)\boldsymbol{i} + (c(t) + d(t)\boldsymbol{i})\boldsymbol{j}, \tag{8}$$

where $\boldsymbol{i}, \boldsymbol{j}, \boldsymbol{k}$ denote the plural units that satisfy

$$\boldsymbol{i}^2 = -1, \quad \boldsymbol{j}^2 = 1, \quad \boldsymbol{k}^2 = 1, \quad \boldsymbol{ij} = \boldsymbol{k}, \quad \boldsymbol{ji} = \boldsymbol{k}, \quad \boldsymbol{jk} = \boldsymbol{i}, \quad \boldsymbol{ki} = -\boldsymbol{j}, \quad \boldsymbol{ik} = -\boldsymbol{j}. \tag{9}$$

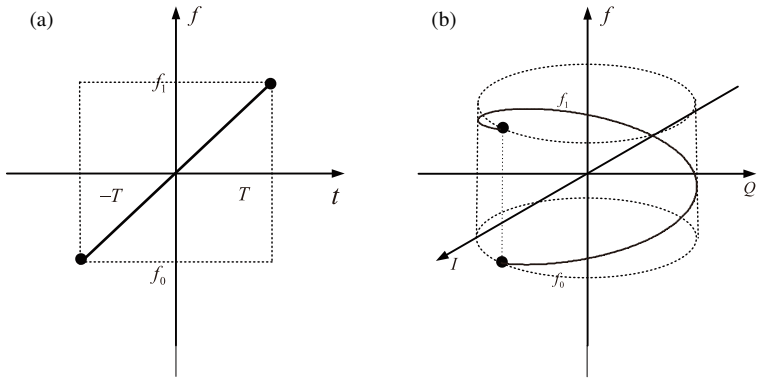

Figure 4 Chirp signal and its 3D expression: (a) chirp signal $f(t) = f_0 + \mu t$; (b) the path of chirp in 3D coordinates.

The Cayley-Dickson algebras offer the possibility to combine the phase modulation and frequency modulation together with the parameters below,

$$S = \boldsymbol{X} + \boldsymbol{Y}\boldsymbol{\mu}, \tag{10}$$

where $\boldsymbol{\mu}$ is either $\boldsymbol{i}$, $\boldsymbol{j}$ or $\boldsymbol{k}$.

According to the waveform design of QFPSK in (5) and the reduced dual quaternion in (7), we use the plural unit $\boldsymbol{\mu} = \boldsymbol{j}$ to represent the frequency modulation. Then, $\boldsymbol{X} = a(t) + b(t)\boldsymbol{i}$ and $\boldsymbol{Y} = c(t) + d(t)\boldsymbol{i}$ represent the phase modulation, while $\boldsymbol{j}$ in $\boldsymbol{X} + \boldsymbol{Y}\boldsymbol{j}$ denotes the frequency modulation. As for the waveform design in (4), the discrete signal $S(n), n = 0, 1, \ldots, N-1$ is expressed by

$$S(n) = a(n) + c(n)\boldsymbol{j}, \tag{11}$$

where the 2 bits Gray code $00, 01, 11, 10$ are transformed to $1, -1, \boldsymbol{j}, -\boldsymbol{j}$. And then, the discrete signal $S(n), n = 0, 1, \ldots, N-1$ for the waveform design in (5) is expressed by

$$S(n) = a(n) + d(n)\boldsymbol{k}, \tag{12}$$

where the 2 bits Gray code $00, 01, 11, 10$ are mapped to $1, -1, \boldsymbol{k}, -\boldsymbol{k}$.

It is obvious that the QFPSK is the basic cell for combined phase and frequency modulation, and can be expressed by the reduced dual quaternion. The extension of QFPSK is the generalized form of traditional constellation mapping, such as PSK and FSK: it is PSK modulation if $\boldsymbol{j}$ is ignored, while it is FSK modulation if $\boldsymbol{i}$ and $\boldsymbol{k}$ are ignored.

3 Spatial extension from QFPSK to Chirp CSK

The MSK signal is treated as a particular offset QPSK (OQPSK) signal with two biased orthogonal symbols, where the most complicated difference is that the envelope is sinusoidal, rather than rectangular. Thus, the MSK signal in IQ plane is the continuous change from the vertex of QPSK, while it is the discrete vertex in the 3D coordinates based on $\boldsymbol{f}$, $\boldsymbol{I}$ and $\boldsymbol{Q}$. Under the generalized orthogonality of 3D coordinates, if $f(t)$ is the continuous frequency, such as the chirp signal in Figure 4(a), the corresponding performance of chirp signal in 3D coordinate is presented in Figure 4(b), where the normalized MED of $f(t)$ is its path around the cylinder. Thus, we use the chirp signal to replace the sine signal and then obtain the continuous change from the vertex of QFPSK in the 3D coordinates, called chirp cyclic shift keying (chirp CSK). Based on the 3D cylindrical coordinate system, the physical meaning expressed in the generalized information geometric space is given as follows to help re-understand the SNR gain of chirp CSK from the spatial structure clearly.

Orthogonal MFSK uses each subcarrier $f_i, i = 1, \ldots, M$ with a narrow bandwidth to realize the whole modulation, which captures a large bandwidth $f_M - f_1$ together. As is known, the demodulation of

MFSK is realized by maximum likelihood estimation with each subcarrier f_i, which loses the gain from the whole bandwidth $f_M - f_1$. How to obtain the gain without loss of the bandwidth efficiency is an interesting problem. The chirp cyclic shift keying just suggests its possibility. The idea of chirp CSK comes from the cyclic code shift keying (CCSK) [2] and pulse position modulation [13]. Here, we use the chirp to modulate the signal with each chirp capturing the whole bandwidth, which results in a gain in SNR and low bit error rate (BER).

3.1 Chirp cyclic shift

Let $s(t) = Ag_T(t)\mathrm{e}^{-\mathrm{j}\cdot\pi K\cdot t^2}$ be a chirp signal with pulse duration T and sampling rate $f_s = B$, where $g_T(t)$ is the pulse shape function with the interval T, bandwidth B, the amplitude A and the sweep rate K. The chirp cyclic shift is first given in the discrete fractional Fourier transform for its implied periodicity. It is assumed that the the discrete form of $s(t)$ is $s(n), n = 0, \ldots, N-1$ and its discrete fractional Fourier transform (FRFT) $S(m)$ satisfies

$$S_\alpha(m) = \sqrt{\frac{\sin\alpha - \mathrm{j}\cos\alpha}{N}}\mathrm{e}^{\mathrm{j}\frac{1}{2}\cot\alpha m^2\Delta u^2}\sum_{n=0}^{N-1}\mathrm{e}^{\mathrm{j}\frac{1}{2}\cot\alpha n^2\Delta t^2}\mathrm{e}^{-\mathrm{j}\frac{2\pi nm}{N}}s(n),\ \ \alpha > 0\ \ \&\ \ \alpha \neq D\pi. \tag{13}$$

According to the sampling theory in Fourier domain, the sampling theory in fractional Fourier domain suggests the chirp periodic extension in time domain and fractional Fourier domain:

$$\begin{aligned} &S_\alpha(m - M\Delta u)\cdot\mathrm{e}^{-\mathrm{j}\frac{1}{2}\cot(m-M)^2\Delta u^2} = S_\alpha(m)\cdot\mathrm{e}^{-\mathrm{j}\frac{1}{2}\cot\alpha m^2\Delta u^2},\\ &s(n - N\Delta t)\mathrm{e}^{\mathrm{j}\frac{1}{2}\cot\alpha(n-N)^2\Delta t^2} = s(n)\mathrm{e}^{\mathrm{j}\frac{1}{2}\cot\alpha n^2\Delta t^2}. \end{aligned} \tag{14}$$

However, $s(n)$ and $S_\alpha(m)$ should be the defined periodic sequence $\widetilde{s}(n)$ and $\widetilde{S}(m)$ within a chirp periodicity in the time domain and fractional domain:

$$\begin{aligned} &S_\alpha(m) = \widetilde{S}_\alpha(m)\cdot R_N(m) = S_\alpha((n))_{\alpha,N}\cdot R_N(m),\\ &s(n) = \widetilde{s}(n)\cdot R_N(n) = s((n))_{\alpha,N}\cdot R_N(n), \end{aligned} \tag{15}$$

where $s((n))_{\alpha,N}$ is chirp periodic extension with length N and

$$R_N(n) = \begin{cases} 1, & 0 \leqslant n \leqslant N-1,\\ 0, & \text{else}, \end{cases}$$

denotes the principal value interval within a periodic sequence.

3.2 Chirp cyclic shift keying modulation

It is assumed that the signal is $s(n) = A\mathrm{e}^{-\mathrm{j}\pi Kn^2\Delta t^2}$ and the time delay is n_τ. The symbol without time delay is $s = [s(0), s(1), \ldots, s(N-2), s(N-1)]$ and the symbol with time delay n_τ and chirp cyclic shift is

$$s_\tau = [\widetilde{s}(-n_\tau), \widetilde{s}(-n_\tau+1), \ldots, \widetilde{s}(0), s(1), \ldots, s(N-n_\tau-1)], \tag{16}$$

where $\widetilde{s}(-n_\tau + n), n = 0, 1, \ldots, n_\tau - 1, n_\tau = 0, \ldots, N-1$ satisfies

$$\widetilde{s}(-n_\tau + n) = s(N - n_\tau + n)\exp\left(\mathrm{j}\frac{1}{2}\cot\alpha(N - n_\tau + n)^2\Delta t^2\right)\exp\left(-\mathrm{j}\frac{1}{2}\cot\alpha(-n_\tau + n)^2\Delta t^2\right). \tag{17}$$

Thus, at the receiver, if the signal is detected by the pulse compression or fractional Fourier transform, the detection value will obtain the BER gain $10\log_{10}(BT)$. Then, we analyze two important indicators of signal modulation: bandwidth efficiency and energy efficiency.

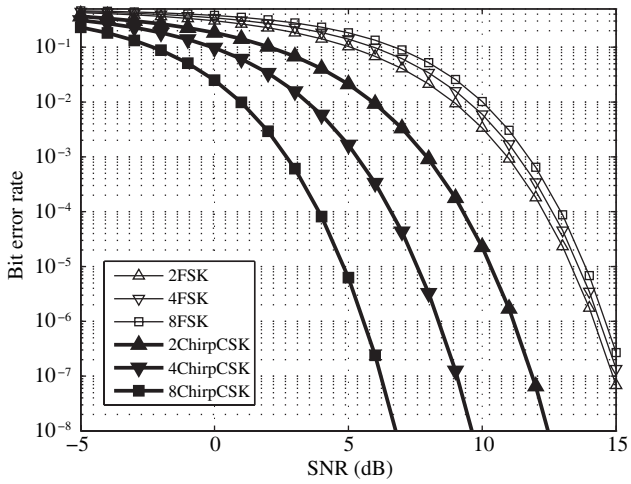

Figure 5 Comparison of M-ary chirp CSK and MFSK: M=2, 4, 8.

3.2.1 *Bandwidth efficiency*

The bandwidth for MFSK is $B_{\mathrm{MFSK}} = (M+1)/T$, yielding the corresponding bandwidth efficiency

$$\eta_{\mathrm{MFSK}} = \frac{\log_2 M}{B_{\mathrm{MFSK}} \cdot T} = \frac{\log_2 M}{M+1}. \tag{18}$$

Since the M-ary chirp cyclic shift modulation, it is assumed that the bandwidth is $B_{\mathrm{MChirpCSK}} = B_{\mathrm{MFSK}} = (M+1)/T$. Then, we have the chirp rate $K = B_{\mathrm{MChirpCSK}}/T = (M+1)/T^2$ and the chirp cyclic shifting points $N = B_{\mathrm{MChirpCSK}}T = M+1$, yielding

$$\eta_{\mathrm{MChirpCSK}} = \frac{\log_2 M}{N} = \frac{\log_2 M}{M+1}. \tag{19}$$

According to Eqs. (18) and (19), the M-ary chirp cyclic shift modulation shares the same bandwidth efficiency with MFSK.

3.2.2 *SNR gain*

Since the pulse compression gain is the time-bandwidth product $G_{\mathrm{MTD}} = B_{\mathrm{MTD}}T = (M+1)/2$, we obtain the SNR gain as $R_{\mathrm{gain}} = 10\log_{10}\left((M+1)/2\right)(\mathrm{dB})$. The symbol error rate of MFSK with noncoherent demodulation is

$$P_{\mathrm{eMFSK}} \approx \frac{M-1}{2}\exp\left(-\frac{r}{2}\right), \tag{20}$$

where the SNR is $r = A^2/(2\sigma^2)$ and $R = 10\log_{10} r = 10\log_{10}\left(A^2/(2\sigma^2)\right)$ in dB. The corresponding BER of MFSK is

$$P_{\mathrm{bMFSK}} = \frac{\frac{M}{2}}{M-1}P_{\mathrm{eMFSK}} \approx \frac{M}{4}\exp\left(-\frac{A^2}{4\sigma^2}\right). \tag{21}$$

Thus, the SNR for the chirp cyclic shift keying modulation is

$$R' = R + R_{\mathrm{gain}} = 10\log_{10}\left(\frac{A^2}{2\sigma^2}\right) + 10\log_{10}(M+1) = 10\log_{10}\left(\frac{C^2}{2\sigma^2}\right)(\mathrm{dB}), \tag{22}$$

with $C = \sqrt{M+1}A$ and $r' = C^2/(2\sigma^2)$. Thus the symbol error rate of Chirp CSK modulation is

$$P_{\mathrm{eMChirpCSK}} \approx \frac{M-1}{2}\mathrm{e}^{-\frac{r'}{2}} = \frac{M-1}{2}\exp\left(-\frac{(M+1)A^2}{4\sigma^2}\right), \tag{23}$$

and the bit error rate (BER) is

$$P_{\mathrm{bMChirpCSK}} = \frac{\frac{M}{2}}{M-1}P_{\mathrm{eMChirpCSK}} \approx \frac{M}{4}\exp\left(-\frac{(M+1)A^2}{4\sigma^2}\right). \tag{24}$$

The BERs of MFSK and M-ary Chirp CSK are given in Figure 5 with $M = 2, 4, 8$. Compared with 2FSK, 4FSK and 8FSK, the 2-ary, 4-ary and 8-ary chirp CSKs obtain 3 dB, 6 dB and 9 dB SNR gain at the BER of 10^{-5}. It is obvious that the Chirp CSK obtains the SNR gain, which is matched with the theoretical analysis in Eqs. (21) and (24).

4 Application in image OFDM system

In the communication system, there is an interesting idea that the constellation modulation shares some similar characteristics with the pixels in an image. As the coding and modulation share some similar characteristics with image, the hypercomplex commutative algebra for color image in [14] was introduced to describe the modulation process in communication. Meanwhile, they explore the extension of these ideas to signals with complex-valued samples, using a quaternion-valued equivalent of the analytic signal obtained from a one-sided quaternion Fourier transform [15]. Besides, in imaging system, image segmentation plays an important role, especially in medical imaging system [16]. These inspire us to use fixed segmented subcarriers to construct the "communication diagram". Then, we divide the signal into parallel subcarriers before the inverse Fourier transform and initially explore its performance with the image properties.

4.1 Image OFDM systems

It is assumed that the size of transmitted image is $M \times N$, which means the number of OFDM symbols is M and the length of each OFDM symbol is N. Thus, the mth OFDM symbol is expressed as

$$\boldsymbol{S}_m = \left[S_m(0), S_m(1), \ldots, S_m(N-1)\right]. \tag{25}$$

Then, the nth subcarrier in the mth OFDM symbol is modulated by the QFPSK $S_m(n) = a(n) + b(n)\boldsymbol{i} + c(n)\boldsymbol{j} + d(n)\boldsymbol{k} = a(n) + d(n)\boldsymbol{k}$. Followed by one dimensional Fourier transform, the modulated symbol is

$$\begin{aligned} s_m(k) &= \frac{1}{\sqrt{N}} \sum_{n=0}^{N-1} S_m(n) \mathrm{e}^{\boldsymbol{i}\frac{2\pi}{N}nk} = \frac{1}{\sqrt{N}} \sum_{n=0}^{N-1} [a(n) + d(n)\boldsymbol{k}] \mathrm{e}^{\boldsymbol{i}\frac{2\pi}{N}nk} \\ &= \frac{1}{\sqrt{N}} \sum_{n=0}^{N-1} a(n) \mathrm{e}^{\boldsymbol{i}\frac{2\pi}{N}nk} + \frac{\boldsymbol{k}}{\sqrt{N}} \sum_{n=0}^{N-1} d(n) \mathrm{e}^{\boldsymbol{i}\frac{2\pi}{N}nk}. \end{aligned} \tag{26}$$

It is noted that if the values of $a(n), d(n)$ satisfy the solid line path in Figure 2(a), the proposed system will be the MSK-OFDM systems.

Based on the aforementioned definition and corollaries, the traditional OFDM system can be regarded as a line by line scan of "image". In the communication system, the two dimensional structure is meaningful to restrain out-bursting noise with the subblock by subblock scan. We produce the updated symbol $\boldsymbol{S}^m$, modulated by traditional MPSK, MQAM and extension of QFPSK, yielding to the image OFDM system in Figure 6.

$$\boldsymbol{S}^m = \begin{bmatrix} S_m(0) & \cdots & S_m(N_1-1) \\ S_m(N_1) & \cdots & S_m(2N_1-1) \\ \vdots & \ddots & \vdots \\ S_m((N_2-1)N_1) & \cdots & S_m(N-1) \end{bmatrix}_{N_2 \times N_1}. \tag{27}$$

The modulation for the mth OFDM symbol is realized by

$$s^m(k_1, k_2) = \frac{1}{\sqrt{N}} \sum_{n_2=0}^{N_2-1} \sum_{n_1=0}^{N_1-1} S^m(n_1, n_2) \mathrm{e}^{\boldsymbol{i}\frac{2\pi}{N_1}n_1k_1 + \boldsymbol{i}\frac{2\pi}{N_2}n_2k_2}, \tag{28}$$

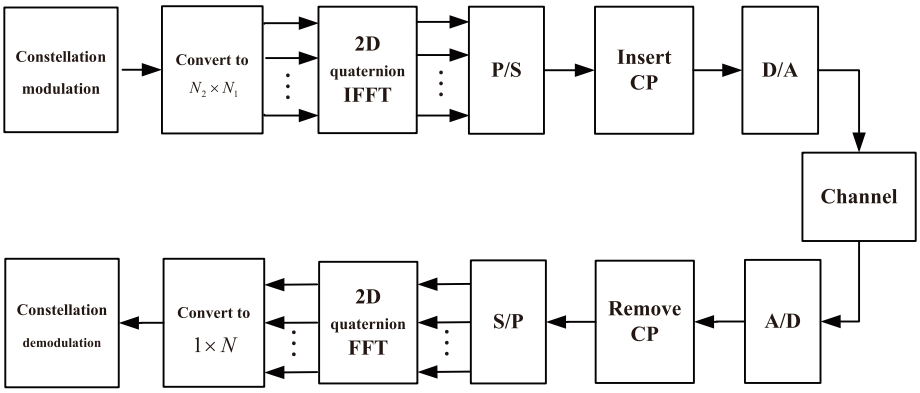

Figure 6 Construction of image OFDM system.

Table 1 Simulation parameters for image OFDM system

Simulation parameters	Values
Num of OFDM symbols	10000
Traditional subcarriers	1024
Parallel subcarriers	32×32
Constellation modulation	QPSK/QFPSK
SNR values	[−5, 15] dB
Channel environment 1	AWGN
Channel environment 2	fast fading with normalized Doppler 0.1
Channel environment 3	frequency selective fading channel
Multipath and fading parameters	[0 3 7 10] and [0 dB −2 dB −14 dB −30 dB]

with $k_1 = 0, 1, \ldots, N_1 - 1$, $k_2 = 0, 1, \ldots, N_2 - 1$ and $m = 1, 2, \ldots, M$. Then, the mth parallel symbol $s^m(k_1, k_2)$ is transmitted in serial mode expressed by

$$\begin{aligned} \boldsymbol{s}^m = [&s^m(0,0), \ldots, s^m(0, N_1 - 1), s^m(1,0), \ldots, s^m(1, N_1 - 1), \ldots, \\ &s^m(N_2 - 1, 0), \ldots, s^m(N_2 - 1, N_1 - 1)]. \end{aligned} \tag{29}$$

In the receiver, the demodulation process is just the inverse process of the above, which is not presented in this paper.

4.2 Performance of QFPSK in image OFDM system

The simulation parameters of proposed OFDM system with different channel environments are given in Table 1. The QPSK in each subcarriers usually contains information with good correlation information, leading to the large peak to average ratio (PAR) in OFDM system. Due to the fact that the QFPSK could be divided into two BPSK modulations in two orthogonal carriers, the QFPSK shares the similar PAPR with BPSK. Meanwhile, the proposed OFDM system with QFPSK is used to decrease the correlation, which results in 0.3 dB lower PAPR at complementary cumulative distribution function (CCDF) 0.01 than that of QPSK in Figure 7. Especially, when the QFPSK is reduced to the MSK (the solid line in Figure 2(a)), it will be the constant envelope OFDM system (CE-OFDM).

In frequency selective fading channel, the comparison of QFPSK and QPSK in 1D OFDM and 2D OFDM systems is presented in Figure 8. In both 1D OFDM and 2D OFDM systems, the BER of QFPSK performs better than that of QPSK. Besides, the simulation also shows that the BER performance of QFPSK in 1D OFDM system is better than that of 2D OFDM system for the former owns large cyclic prefix to combat the multi-path effect.

The simulation of the proposed OFDM system in the time-varying wireless channel with normalized Doppler 0.1 is depicted in Figure 9. We can see that the bit error probability of proposed OFDM system is below 0.1 while that of the traditional one is about 0.25 at the SNR of 15 dB. The QFPSK performs

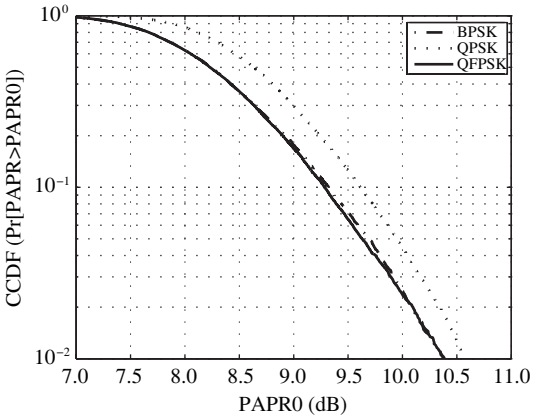

Figure 7 The comparison of PAPR in OFDM system.

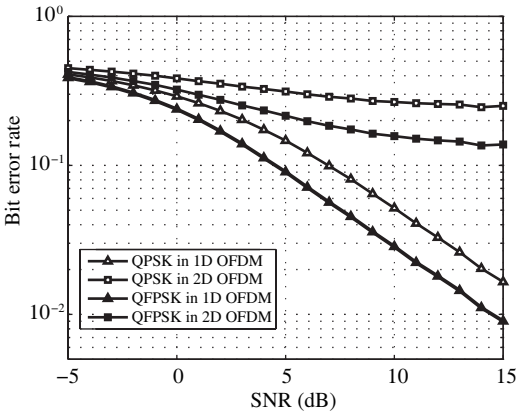

Figure 8 Performance in frequency selective fading channel.

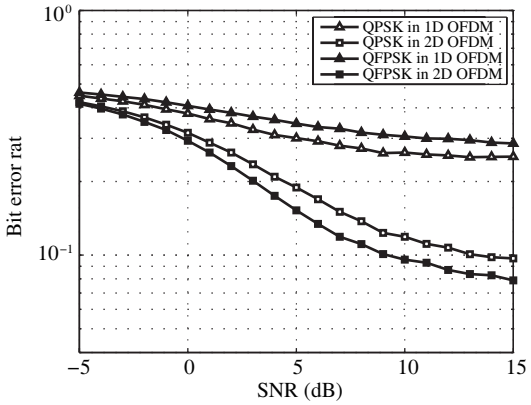

Figure 9 Performance in fast time-varying channel with normalized Doppler 0.1.

better than the QPSK in the proposed OFDM system, while the situation is opposite in the traditional OFDM systems. The result proves the robustness of proposed system against the Doppler spread in the time-varying wireless channel.

5 Conclusion

In this paper, the generalized spatial representation for combined frequency and phase constellation mapping is redefined in the 3D coordinates based on $\boldsymbol{f}, \boldsymbol{I}, \boldsymbol{Q}$. The reduced dual quaternion is adopted as the mathematical expression for the basic combined frequency and phase modulation called quadrature frequency-phase shift keying (QFPSK). As a special case of QFPSK, the symbol error rate of MSK is first given based on the 3D coordinate. Then, the spatial extension from QFPSK to Chirp CSK is given with the time-bandwidth gain BT. At last, the QFPSK is combined with the 2D OFDM system, yeilding the image OFDM system. Simulation results show that the QFPSK obtains lower PAR and keeps its robustness against the fast time-varying channel in the image OFDM system.

Acknowledgements This work was supported in part by National Natural Science Foundation of China (Grant Nos. 61501051, 61421001), and Ph.D. Programs Foundation of Ministry of Education of China (Grant No. 20121101130001).

Conflict of interest The authors declare that they have no conflict of interest.

References

1 Proakis J G, Salehi M. Digital Communications. 5th ed. New York: McGraw-Hill, 2007. 227–229
2 Hu S, Bi G A, Guan Y L, et al. Spectrally efficient transform domain communication system with quadrature cyclic code shift keying. IET Commun, 2013, 7: 382–390
3 Kang S G, Chen Z, Kim J Y, et al. Construction of higher-level 3-D signal constellations and their accurate symbol error probabilities in AWGN. IEEE Trans Signal Process, 2011, 59: 6267–6272
4 Boutros J, Viterbo E. Signal space diversity: a power- and bandwidth-efficient diversity technique for the Rayleigh fading channel. IEEE Trans Inf Theory, 1998, 44: 1453–1467
5 Saha D, Birdsall T G. Quadrature-quadrature phase-shift keying. IEEE Trans Commun, 2010, 37: 437–3409
6 Kang S G. An OFDM with 3D signal mapper and IDFT modulator. IEEE Commun Lett, 2008, 12: 871–873
7 Lee H, Paulraj A. MIMO systems based on modulation diversity. IEEE Trans Commun, 2010, 58: 3405–3409
8 Cheng S, Seshadri R I, Valenti M C, et al. The capacity of noncoherent continuous-phase frequency shift keying. In: Proceedings of the 41st Annual Conference on Information Sciences and Systems, Baltimore, 2007. 396–401
9 Cheng S, Valenti M C, Torrieri D. Coherent continuous-phase frequency-shift keying: parameter optimization and code design. IEEE Trans Wirel Commun, 2009, 8: 1792–1802
10 Shi P F, Huan H, Tao R. Waveform design for higher-level 3D constellation mappings and its construction based on regular tetrahedron cells. Sci China Inf Sci, 2015, 58: 082302
11 Chen Z, Choi E C, Kang S G. Closed-form expressions for the symbol error probability of 3D OFDM. IEEE Commun Lett, 2010, 14: 112–114
12 Liu W. Antenna array signal processing for a quaternion-valued wireless communication system. In: Proceedings of the IEEE Benjamin Franklin Symposium on Microwave and Antenna Sub-systems (BenMAS), Philadelphia, 2014. 1–3
13 Ma X, Wang S, Zhang S, et al. High bit rate pulse position modulation signal generation based on rare-earth-doped crystals. IEEE Commun Lett, 2015, 19: 179–182
14 Ell T A, Sangwine S J. Hypercomplex Fourier transforms of color image. IEEE Trans Image Process, 2007, 16: 22–35
15 Le B N, Sangwine S J, Ell T A. Instantaneous frequency and amplitude of orthocomplex modulated signals based on quaternion Fourier transform. Signal Process, 2014, 94: 308–318
16 Wang L F, Yu Z Y, Pan C H. A unified level set framework utilizing parameter priors for medical image segmentation. Sci China Inf Sci, 2013, 56: 110902